Characterization and Kinetics of Phosphopantothenoylcysteine Synthetase from *Enterococcus faecalis*[†]

Jiangwei Yao, James D. Patrone, and Garry D. Dotson*

Department of Medicinal Chemistry, College of Pharmacy, University of Michigan, Ann Arbor, Michigan 48109-1065

Received December 8, 2008; Revised Manuscript Received January 27, 2009

ABSTRACT: The enzyme phosphopantothenoylcysteine synthetase (PPCS) catalyzes the nucleotide-dependent formation of phosphopantothenoylcysteine from (*R*)-phosphopantothenate and L-cysteine in the biosynthetic pathway leading to the formation of the essential biomolecule, coenzyme A. The *Enterococcus faecalis* gene *coaB* encodes a novel monofunctional PPCS which has been cloned into pET23a and expressed in *Escherichia coli* BL21 AI. The heterologous expression system yielded 30 mg of purified PPCS per liter of cell culture. The purified enzyme chromatographed as a homodimer of 28 kDa subunits on Superdex HR 200 gel filtration resin. The monofunctional protein displayed a nucleotide specificity for cytidine 5′-triphosphate (CTP) analogous to that seen for bifunctional PPCS expressed by most prokaryotes. Kinetic characterization, utilizing initial velocity and product inhibition studies, found the mechanism of PPCS to be Bi Uni Uni Bi Ping-Pong, with the nucleotide CTP binding first and CMP released last. Michaelis constants were 156, 17, and 86 μM for CTP, (*R*)-phosphopantothenate, and L-cysteine, respectively, and the k_{cat} was 2.9 s^{-1}. [*carboxyl*-^{18}O]Phosphopantothenate was prepared by hydrolysis of methyl pantothenate with Na^{18}OH, followed by enzymatic phosphorylation with *E. faecalis* pantothenate kinase (PanK). The fate of the carboxylate oxygen of labeled phosphopantothenate, during the course of the PPCS-catalyzed reaction with CTP and L-cysteine, was monitored by ^{31}P NMR spectroscopy. The results show that the carboxylate oxygen of the phosphopantothenate is recovered with the CMP formed during the reaction, indicative of the formation of a phosphopantothenoyl cytidylate catalytic intermediate, which is consistent with the kinetic mechanism.

Phosphopantetheine ((*R*)-3-hydroxy-4-(3-(2-mercaptoethylamino)-3-oxopropylamino)-2,2-dimethyl-4-oxobutyl dihydrogen phosphate) is an fundamental feature in many biological acyl transfer reactions (*1*−*3*). The molecule is found imbedded within coenzyme A (CoA),[1] as well as on a posttranslationally modified, conserved serine of acyl carrier protein (ACP) (*1*). Both CoA and ACP play essential roles in activating various acyl groups for enzyme-catalyzed transfer in several reactions associated with intermediary metabolism and cell membrane assembly in living organisms (*4*). The critical nature of phosphopantetheine-containing molecules to the integrity and viability of cells makes the biosynthetic pathway leading to the production of these compounds an intriguing target for antimicrobial development (*5, 6*).

While it has been known for decades that CoA is biosynthesized from nucleoside triphosphate (NTP), D-pantothenate, and L-cysteine, the genes involved have only been identified in recent years (*7*−*9*). In eukaryotic systems that have been characterized, the phosphopantetheine portion of CoA is synthesized from pantothenate via three chemical reactions catalyzed by three polypeptides (Scheme 1) (*10*). First, pantothenate is phosphorylated by pantothenate kinase (PanK; EC 2.7.1.33; *coaA*), using ATP as the phosphate donor, to yield phosphopantothenate (PPA). This is followed by amide bond formation between the carboxyl group of PPA and the amino group of L-cysteine catalyzed by an ATP-dependent phosphopantothenoylcysteine synthetase (PPCS; EC 6.3.2.5; *coaB*). Subsequent decarboxylation of the carboxylic acid moiety on the ligated cysteine of phosphopantothenoylcysteine by phosphopantothenoylcysteine decarboxylase (PPCDC; EC 4.1.1.36; *coaC*) gives 4′-phosphopantetheine. In bacterial systems elucidated so far, the second and third chemical steps, the ligation and decarboxylation of cysteine by PPCS and PPCDC, are catalyzed by a single bifunctional polypeptide (*9, 11*). Furthermore, CTP, rather than ATP, is required by the bifunctional PPCS (*7, 9*).

PPCS from few species have been characterized. The proposed mechanism of PPCS involves the formation of an acyl cytidylate intermediate, 4′-phosphopantothenoyl cytidylate, between the carboxylate moiety of D-pantothenate and the α-phosphate of CTP, with the concomitant release of pyrophosphate. Formation of the product occurs by

[†] This research was supported by the University of Michigan, College of Pharmacy. J.Y. was supported in part by a U.S. Department of Homeland Security Fellowship administered by the Oak Ridge Institute for Science and Education. J.D.P. was supported in part by a National Institutes of Health Chemistry and Biology Interface Training Grant.

* To whom correspondence should be addressed. Phone: (734) 615-6543. Fax: (734) 647-8430. E-mail: gdotson@umich.edu.

[1] Abbreviations: ACP, acyl carrier protein; ATP, adenosine 5′-triphosphate; CoA, coenzyme A; CTP, cytidine 5′-triphosphate; DTT, dithiothreitol; ESI-MS, electrospray ionization−mass spectroscopy; HEPES, 4-(2-hydroxyethyl)-1-piperazineethanesulfonic acid; NADH, nicotinamide adenine dinucleotide; PanK, pantothenate kinase; PPA, phosphopantothenate; PPCDC, phosphopantothenoylcysteine decarboxylase; PPCS, phosphopantothenoylcysteine synthetase; PP_i, pyrophosphate; PP_i-FPK, pyrophosphate-dependent fructose-6-phosphate kinase; SDS−PAGE, sodium dodecyl sulfate−polyacrylamide gel electrophoresis; Tris, tris(hydroxymethyl)aminomethane.

10.1021/bi802240w CCC: $40.75
Published on Web 01/30/2009

Scheme 1

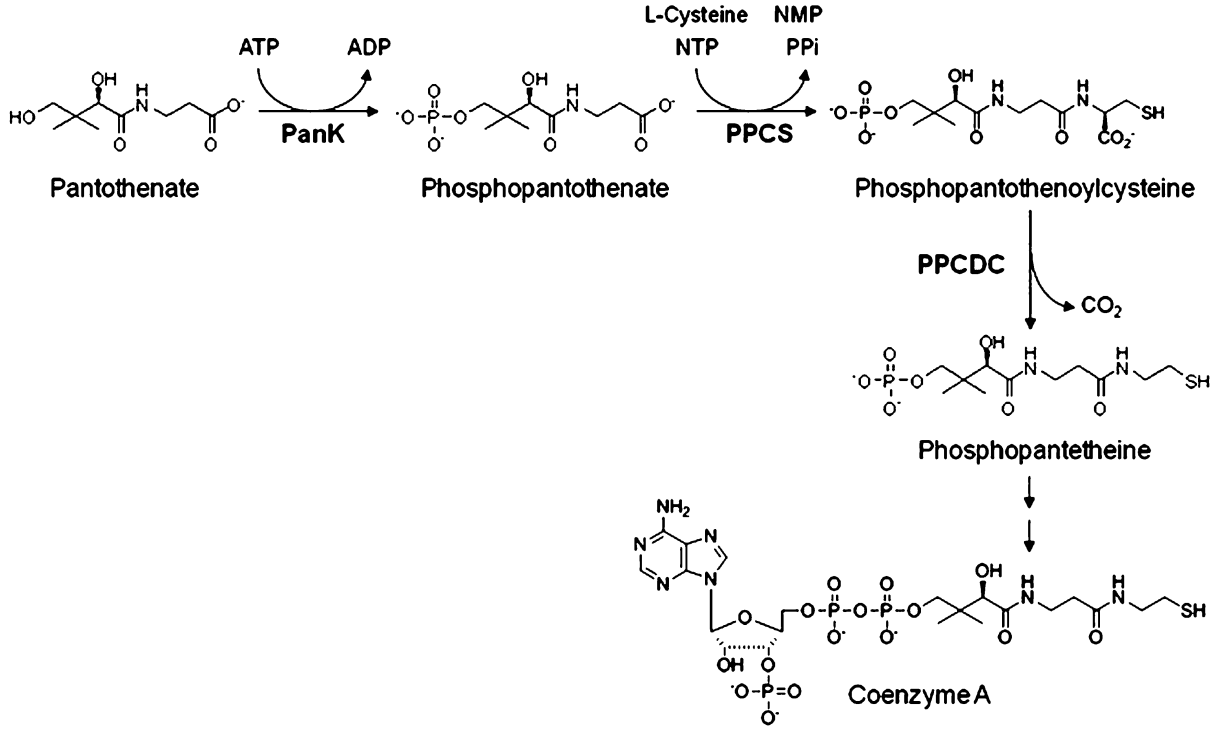

transfer of the nucleotide-activated acyl group to the amino group of L-cysteine, yielding phosphopantothenoylcysteine and CMP (Scheme 2). This proposed mechanism is supported by structural studies on the *E. coli* N210D PPCS domain, where the acyl cytidylate intermediate was observed in the active site when the crystal of the mutated PPCS was soaked with CTP and PPA (*12*). However, there has been no complete study on the kinetic mechanism of PPCS. In this paper, we overexpress, purify, and characterize PPCS from *Enterococcus faecalis*, which unlike most other bacterial PPCS is encoded as a monofunctional protein and has similarly distant homology from both the monofunctional human PPCS protein and bifunctional bacterial PPCS domains (*5, 10*). In this study we use initial velocity and product competition experiments to elucidate the kinetic mechanism of PPCS from *E. faecalis* and report for the first time the chemical mechanism and nucleotide specificity of a monofunctional bacterial PPCS.

Scheme 2

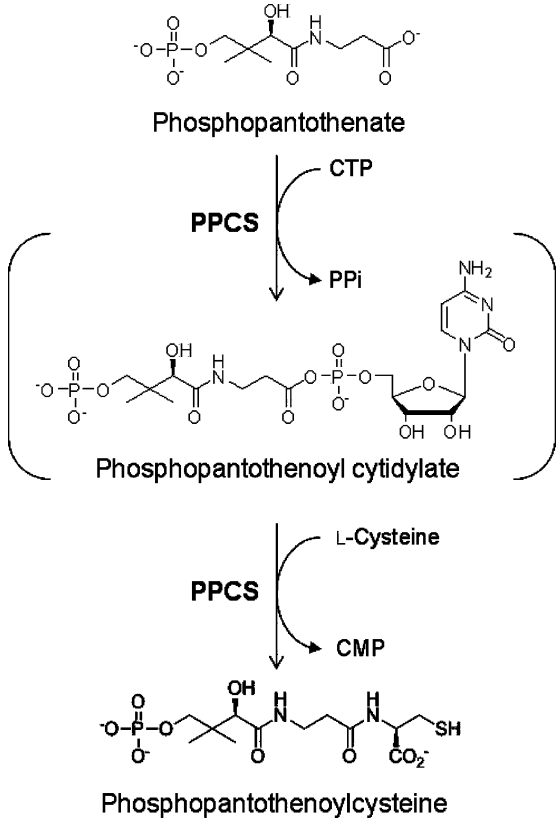

MATERIALS AND METHODS

Materials. The chemicals used were of reagent grade or of the highest purity commercially available and were not further purified. Source 15Q, Source 15S, and Superdex 200 were from GE Healthcare. Calcium D-pantothenate, HEPES, Tris base, ATP, CTP, pyrophosphate reagent, ampicillin, sodium chloride, sodium hydroxide, methanol, formic acid, sodium pyrophosphate, dithiothreitol, L-cysteine, and 97% [^{18}O]water were from Sigma-Aldrich. Lauria agar (Lennox) and Lauria broth (Lennox) were from Difco. Restriction and DNA modifying enzymes were from New England Biolabs. The *Escherichia coli* BL21 AI was obtained from Invitrogen, and *E. coli* XL1 Blue was obtained from Stratagene. Polymerase chain reaction was performed using an Eppendorf gradient mastercycler and *Pfu*Turbo hotstart DNA polymerase (Stratagene). Oligonucleotides were synthesized by Invitrogen. Qiagen minispin kits were used for DNA purification and PCR reaction cleanup. Electrospray mass spectral analysis was performed at the University of Michigan Mass Spectrometry Facility, Department of Chemistry. DNA sequencing was performed by the University of Michigan, Biomedical Research Resources Core Facility.

Cloning, Overexpression, and Purification of E. faecalis PPCS. The *coaB*gene was amplified from *E. faecalis* genomic DNA (strain ATCC 700802), via PCR, using the forward primer GCGCCATATGGATGTTTTAGTTACTGCTGGCGG and the reverse primer GCGCCTCGAGTCATTGTTGTTCTCTCCATTTCTTTTC to introduce an *Nde*I site (shown underlined) upstream of the gene and an *Xho*I site downstream of the gene. The resulting PCR product, encoding the entire *coaB* gene, was digested with *Nde*I and *Xho*I and ligated into pET23a(+) (Novagen) which had been restricted with *Nde*I and *Xho*I. The desired plasmid was designated pUMGD1, and the insert was confirmed by DNA sequencing. *E. coli* strain BL21 AI harboring the plasmid pUMGD1 was incubated in four 1 L flasks containing 250 mL each of LB−ampicillin media (5 g of NaCl, 5 g of yeast extract, 10 g of tryptone, and 100 mg of ampicillin per liter) at 37 °C with vigorous shaking (250 rpm) until the optical density at 600 nm reached 0.6−0.8. The culture was cooled to 17 °C and induced with a final concentration of 0.065% (w/v) L-arabinose. Incubation (17 °C, 250 rpm) was continued overnight. Cells from the 1 L of culture were harvested by centrifugation at 10000*g*, washed with 20 mM HEPES, pH 8.0, and suspended in 80 mL of 20 mM HEPES, pH 8.0. The cells were disrupted by French press, and the resulting suspension was centrifuged at 20000*g* for 30 min to separate the crude cytosol (supernatant) from cellular debris (pellet). The cytosol was chromatographed on a Source 15Q column (8 mL of resin per 250 mL of cell culture) equilibrated with 20 mM HEPES, pH 8.0, washed with 3 column volumes of equilibration buffer, and eluted with a 10 column volume linear gradient of 0−0.5 M NaCl in 20 mM HEPES, pH 8.0. Fractions were analyzed by SDS−PAGE, and fractions containing PPCS were pooled and passed through a 320 mL Superdex 200 prep grade column equilibrated in 20 mM HEPES, pH 8.0, containing 150 mM NaCl. The purified fractions were dialyzed against 20 mM HEPES, pH 8.0, and stored at −80 °C.

Cloning, Overexpression, and Purification of the Pyrophosphate-Dependent Fructose-6-phosphate Kinase (PP_i-FPK). The *E. coli* codon optimized PP_i-PFK gene (DNA 2.0) of *Propionibacterium freudenreichii*, containing a *Nde*I site upstream and a *Xho*I site downstream of the gene, was digested with *Nde*I and *Xho*I and ligated into pET23a(+) via the same sites (*13*). The resulting vector was designated pUMJY901. Growth, expression, and purification protocols used were the same as for PPCS (above).

High-Resolution Mass Spectrometry. The purified *E. faecalis* PPCS was dialyzed against H_2O and brought to 50/50 methanol/water containing 1% formic acid. The sample (final protein concentration of 0.2 mg/mL) was submitted for positive-ion ESI-MS.

Synthesis of 4′-Phosphopantothenate. 4′-Phosphopantothenate was synthesized via previously published procedures (*9*).

Synthesis of [carboxyl-^{18}O]Phosphopantothenate. Methyl D-pantothenate (18.6 mg, 80 μmol) was treated with 0.4 M $Na^{18}OH$ in 200 μL final volume (8 μL of 10 M NaOH and 192 μL of 97% $H_2{}^{18}O$ for a final concentration of 93.2% ^{18}O) for 2 h at room temperature. The reaction was then neutralized by applying to an AG MP-50 resin spin column (H^+ form; 1 mL) and centrifuging at 1000*g* for 2 min to yield [*carboxyl*-^{18}O]-D-pantothenate. The labeled pantothenate was then converted, biochemically, into [*carboxyl*-^{18}O]-D-phosphopantothenate by incubating at 30 °C overnight in the presence of 1.1 equiv of ATP and 10 μM *E. faecalis* pantothenate kinase in 50 mM HEPES, pH 8.0 (5 mL final volume). The reaction was separated on a Source 15Q column (8 mL) via a linear gradient elution of 0−0.4 M NaCl in water. Fractions containing labeled phosphopantothenate, detected enzymatically using the PPCS assay (described below), were combined and lyophilized. The lyophilized fractions were subjected to gel filtration on a Bio-Gel P-2 column (240 mL) in water to remove NaCl. The relevant fractions were lyophilized and characterized. ^{1}H NMR (500 MHz, D_2O): δ 0.82 (s, 3H), 0.99 (s, 3H), 2.41 (t, 2H), 3.39 (dd, 1H), 3.42 (dt, 2H), 3.75 (dd, 1H), 4.1 (s, 1H). ^{13}C NMR (125 MHz, D_2O): δ 17.96 (s), 21.42 (s), 36.12 (s), 36.72 (s), 38.35 (d), 70.69 (d), 74.77 (s), 174.76 (s), 180.268 (s, caboxylate ^{18}O), 180.295 (s, caboxylate ^{16}O); ratio of carboxylate species 92 to 10 (^{18}O to ^{16}O).

^{18}O Transfer Reaction. A reaction mixture of 10 mM CTP, 10 mM $MgCl_2$, 12 mM [*carboxyl*-^{18}O]-D-phosphopantothenate, 10 mM L-cysteine, 10 mM DTT, and 2.4 μM *E. faecalis* PPCS in 500 μL of 100 mM Tris-HCl, pH 7.6, was incubated for 1 h at 37 °C. The reaction was then filtered through a Microcon YM-10 membrane (Amicon) at 13000*g* and 15 °C for 30 min to remove the enzyme. To the filtrate was added 120 μL of ^2H_2O, and the solution was analyzed via ^{31}P NMR. Analogous control experiments with unlabeled D-phosphopantothenate or without enzyme were also performed.

NMR Spectroscopy. Proton-decoupled ^{31}P NMR spectra were recorded on a Bruker DRX500 spectrometer (11.75 T) at a probe temperature of 298 K, tuned to 202.4 MHz, using 5 mm high-resolution NMR tubes. Spectra were obtained with a spectral width of 80000 Hz, 1.0 s relaxation delay, and 32768 complex points in the time domain using simultaneous detection of real and imaginary components. The time domain data were apodized with an exponential (0.5 Hz) prior to zero-filling followed by Fourier transformation. Chemical shifts are reported relative to an external sample of 10 mM inorganic phosphate (0.0 ppm) in 100 mM Tris-HCl (pH 7.6) and 10% ^2H_2O.

Proton-decoupled ^{13}C NMR spectra were recorded on a Bruker DRX500 spectrometer (11.75 T) at a probe temperature of 298 K, tuned to 125.7 MHz, using 5 mm high-resolution NMR tubes. Spectra were obtained with a spectral width of 25000 Hz, 1.0 s relaxation delay, and 32768 complex points in the time domain using simultaneous detection of real and imaginary components. The time domain data were apodized with an exponential (0.5 Hz) prior to zero-filling followed by Fourier transformation. Chemical shifts are reported relative to tetramethylsilane (0.0 ppm).

Enzyme Assay. The PPCS reaction was observed in the forward reaction via an enzyme-linked assay, where the production of pyrophosphate from PPCS activity was coupled to the oxidation of NADH, which could be monitored as a disappearance of absorption at 340 nm. All of the components of the pyrophosphate detection system are available commercially as the pyrophosphate reagent (PR) from Sigma-Aldrich. It was necessary that additional units of PP_i-PFK be added to the commercial preparation in order to use it as a continuous assay. With this modification PPCS activity could be observed in real time under our experimental

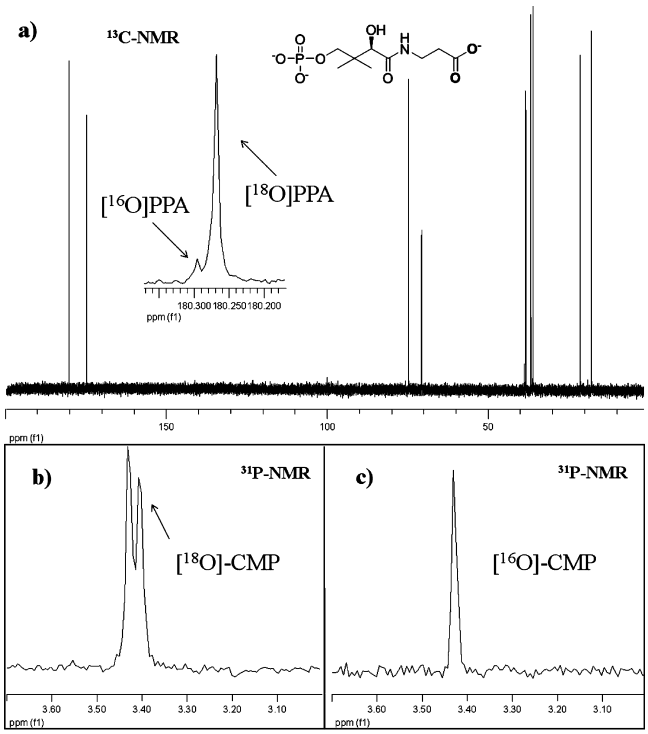

FIGURE 1: ^{13}C and ^{31}P NMR spectra. (a) ^{13}C NMR (proton-decoupled) spectrum of [*carboxyl*-^{18}O]phosphopantothenate. (b) ^{31}P NMR (proton-decoupled) spectrum of CMP produced during PPCS catalysis using [*carboxyl*-^{18}O]phosphopantothenate. (c) ^{31}P NMR (proton-decoupled) spectrum of CMP produced during PPCS catalysis using unlabeled phosphopantothenate. Experimental details are listed under Materials and Methods.

conditions. The assays were performed on a SpectraMax M5 (Molecular Devices) microplate reader using 96-well half-area plates (Costar UV), where each assay has 100 μL final volume. Each vial of the PR was resuspended in 4.5 mL of 100 mM HEPES, pH 7.6. The assay mix consisted of 30 μL of PR, 1 unit of additional PP_i-PFK, 10 mM DTT, and varying concentrations of the substrates (CTP, L-cysteine, and PPA) in a volume of 70 μL buffered in 50 mM Tris-HCl and pH 7.6. All assay mixes contained $MgCl_2$ in 1:1 molar stoichiometry with nucleoside triphosphate. The assay mix and the enzyme solution (275 nM PPCS in 50 mM Tris-HCl, pH 7.6) were incubated at 37 °C for 15 min before the assay. Reactions were initiated by adding 30 μL of enzyme solution to the assay mix. The oxidation of NADH, monitored by a decreasing UV absorbance at 340 nm ($\epsilon = 6.22$ mM^{-1} cm^{-1}), is measured over the course of the assay, and the activity of the enzyme is calculated by adjusting for path length (0.5 cm) and taking into account that each mole of pyrophosphate produced leads to the oxidation of 2 mol of NADH. Assays were run in duplicates, with the average velocities reported.

Initial Velocity Studies. Pairwise analyses, where initial velocities were measured with varying concentrations of one substrate at different fixed concentrations of a second substrate while holding the third substrate at saturation, were conducted. For instance, initial velocities as a function [CTP] were measured at several fixed levels of [PPA] (0.6, 0.3, 0.15, 0.075, and 0.0375 mM) with a constant level of [cysteine] (1 mM). Pairwise analyses were performed for all three substrates.

Product Inhibition Studies. Initial velocities were measured against different concentrations of one substrate with fixed concentrations of the other two substrates and different fixed concentrations of the product inhibitor. For example, initial velocities versus [CTP] were measured at 0.15 mM PPA, 1 mM cysteine, and several fixed levels of [CMP] (0, 250, 500, and 1000 μM).

Data Analysis. Initial velocity was first graphically analyzed as Lineweaver−Burk double-reciprocal plots. Velocity versus the varying [substrate] data was fit to eq 1 to determine the K_m^{app} and k_{cat}^{app}, which was in turn used to derive the fitting lines in the Lineweaver−Burk plots. The different patterns in the Lineweaver−Burk plots arising from the pairwise or inhibition analysis were used to determine which terreactant kinetic mechanism describes PPCS. The initial velocity data from the three sets of pairwise analysis were fit to the initial velocity equation (eq 2) describing the appropriate mechanism (Bi Uni Uni Bi Ping-Pong) to determine the relevant kinetic parameters. Likewise, product inhibition data were fitted to the appropriate product inhibition equations (eqs 3−5) to determine the relevant kinetic parameters.

$$v = \frac{V_{max}^{app}[A]}{K_m^{app} + [A]} \tag{1}$$

$$v = \frac{V_{max}[A][B][C]}{K_{ia}K_{mB}[C] + K_{mC}[A][B] + K_{mB}[A][C] + K_{mA}[B][C] + [A][B][C]} \tag{2}$$

$$v = \frac{V_{max}[A]}{K_{mA}\left(1 + \frac{K_{ia}K_{mB}}{K_{mA}[B]} + \frac{K_{ia}K_{mB}[R]}{K_{mA}K_{ir}[B]} + \frac{[R]}{K_{ir}}\right) + [A]\left(1 + \frac{K_{mB}}{[B]} + \frac{K_{mC}}{[C]}\right)} \tag{3}$$

$$v = \frac{V_{max}[B]}{K_{mB}\left(1 + \frac{K_{ia}}{[A]} + \frac{K_{ia}[R]}{K_{ir}[A]}\right) + [B]\left(1 + \frac{K_{mA}}{[A]} + \frac{K_{mC}}{[C]} + \frac{K_{mA}[R]}{K_{ir}[A]}\right)} \tag{4}$$

$$v = \frac{V_{max}[C]}{K_{mC} + [C]\left(1 + \frac{K_{mA}}{[A]} + \frac{K_{mB}}{[B]} + \frac{K_{ia}K_{mB}}{[A][B]} + \frac{K_{ia}K_{mB}[R]}{K_{ir}[A][B]} + \frac{K_{mA}[R]}{K_{ir}[A]}\right)} \tag{5}$$

In these equations v is initial velocity and V_{max} is maximum velocity. K_{mA}, K_{mB}, and K_{mC} are the Michaelis constants for substrates A, B, and C, respectively. K_{ia} is the dissociation constant of substrate A, and K_{ir} is the inhibition constant of the product R.

RESULTS

Protein Expression and Purification of Recombinant E. faecalis PPCS. PPCS is eluted from the Source 15Q anion-exchange column at 200 mM NaCl. After anion-exchange and gel filtration chromatography the synthetase was >98% pure as determined by SDS−PAGE. Approximately 30 mg of soluble, purified PPCS was obtained per liter of cell culture, with a specific activity of 5.2 units/mg. The native oligomerization state of PPCS was determined via gel filtration. The elution volume of the synthetase on a Superdex

200 HR column was compared to the elution volumes of known protein standard (Bio-Rad gel filtration standard) in order to determine its apparent molecular weight. PPCS eluted as an ~60 kDa molecule, suggestive of a homodimer (theoretical mass 57 kDa).

The purified protein was further analyzed by positive ion ESI-MS and found to have a molecular mass of 28415.0 Da. This mass corresponds to the calculated mass of the recombinant protein (28525.2 Da) associating with one molecule of sodium (23 Da) minus the amino-terminal methionine (133.2 Da). The mass shows that *E. faecalis* PPCS has no attached prosthetic group, in agreement with previous studies performed on the *E. coli* synthetase (*9*).

ATP/CTP Specificity of E. faecalis PPCS. Since the amino acid homology of *E. faecalis* PPCS is equally divergent from both human and *E. coli* PPCS, it was unclear whether the *E. faecalis* enzyme would be ATP or CTP selective. To determine its nucleotide specificity, the *E. faecalis* enzyme was assayed in the presence of either 10 mM ATP or CTP, 0.6 mM PPA, and 1 mM cysteine, representing saturating conditions for all substrates (particularly CTP, which is present at a concentration approximately 65 times its determined K_m). Under these conditions, the ATP-containing reaction showed only 8% of the activity of the CTP-containing reaction, suggesting that the *E. faecalis* enzyme is highly selective for CTP like other bacterial PPCS.

Oxygen Transfer during PPCS Catalysis. Figure 1a shows the ^{13}C NMR spectrum of [*carboxyl*-^{18}O]PPA synthesized by hydrolysis of methyl phosphopantothenate with $Na^{18}OH$ (93% ^{18}O). The inset shows two NMR resonances separated by 0.027 ppm, which correspond to [*carboxyl*-^{16}O]PPA and [*carboxyl*-^{18}O]PPA, and integrate to a ratio of 1 to 9.2, respectively. Thus, the labeled PPA contains 90% ^{18}O distributed between the two carboxylate oxygens, consistent with the percentage of ^{18}O (93%) contained in the saponification reaction. This compound was used as a substrate for the *E. faecalis* PPCS reaction to confirm the formation of a phosphopantothenoyl cytidylate intermediate. Figure 1b depicts the ^{31}P NMR spectra of CMP formed during the PPCS-catalyzed reaction. Two NMR resonances separated by 0.025 ppm were seen corresponding to CMP labeled with no and one ^{18}O atom. The upfield-shifted ^{18}O-labeled CMP resonance represents approximately 45% of the total CMP resonances, which is what would be expected from the transfer of one of the two equivalent carboxylate oxygens of PPA. The ^{31}P NMR of the control reaction (Figure 1c), in which unlabeled PPA was used as a substrate for PPCS, shows a single resonance corresponding to unlabeled CMP. From these results it was determined that the *E. faecalis* PPCS-catalyzed reaction proceeds through the formation of a phosphopantothenoyl cytidylate intermediate.

Enzyme Mechanism. In the double-reciprocal plot of initial velocity against [CTP] at various [PPA] with saturating [cysteine], the fitted lines intersect to the left of the *y*-axis. Replots of intercept vs 1/[PPA] and slope vs 1/[PPA] both have a good linear fit (Figure 2). Thus, CTP and PPA are sequential with respect to each other, so in the overall mechanism both CTP and PPA must bind to the enzyme before a chemical reaction can occur. In the double-reciprocal plot of initial velocity against [cysteine] at various [PPA], the fitted lines are parallel, with replot of intersect vs 1/[PPA] having a good linear fit, consistent with a mechanism where

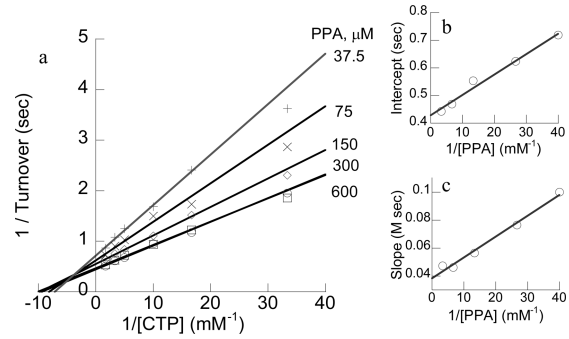

FIGURE 2: Pairwise analysis of CTP and PPA. Initial velocity analysis of PPCS with varying [CTP] and [PPA] at 1 mM cysteine. (a) Double-reciprocal plot of velocity data. (b) Secondary plot of intercepts versus reciprocal [PPA]. (c) Secondary plot of slope versus reciprocal [PPA].

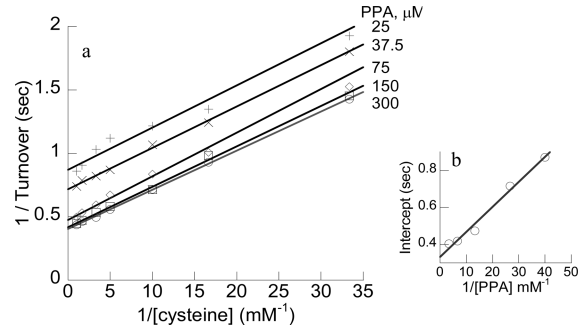

FIGURE 3: Pairwise analysis of cysteine and PPA. Initial velocity analysis of PPCS with varying [cysteine] and [PPA] at 0.6 mM CTP. (a) Double-reciprocal plot of velocity data. (b) Secondary plot of intercepts versus reciprocal [PPA].

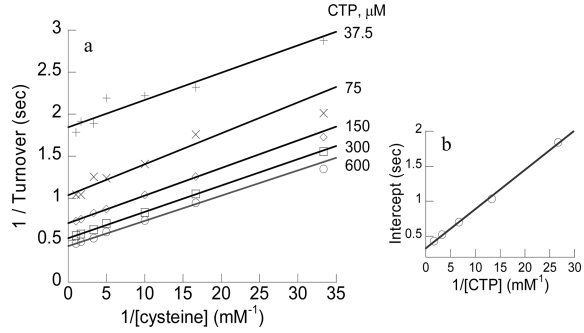

FIGURE 4: Pairwise analysis of cysteine and CTP. Initial velocity analysis of PPCS with varying [cysteine] and [CTP] at 0.6 mM PPA. (a) Double-reciprocal plot of velocity data. (b) Secondary plot of intercepts versus reciprocal [CTP].

PPA and cysteine are Ping-Pong with respect to each other (Figure 3). Thus, in the overall mechanism, there is a product release step between the binding of PPA and the binding of cysteine. Likewise, in the double-reciprocal plot of initial velocity against [cysteine] at various [CTP], the fitted lines are parallel again, with a linear fit in the replot of intersect vs 1/[CTP], consistent with a mechanism where PPA and CTP are Ping-Pong with respect to each other (Figure 4). Again, in the overall mechanism, there is a product release step between the binding of CTP and the binding of cysteine. Given that CTP and PPA must both bind to the enzyme before the first half-reaction occurs, the only terreactant mechanism consistent with the data is the Bi Uni Uni Bi Ping-Pong mechanism.

The product inhibition pattern of CMP with respect to the three substrates is examined to determine the sequence of

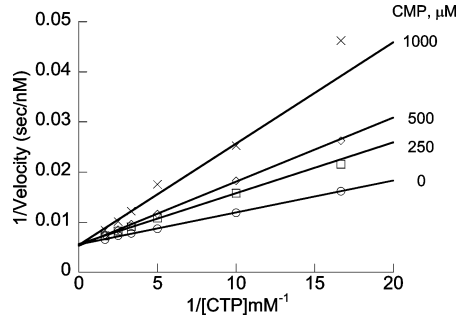

FIGURE 5: Product inhibition analysis of CMP versus CTP. Initial velocity analysis of PPCS versus varying [CTP] at different fixed [CMP] with 0.15 mM PPA and 1 mM cysteine. Double-reciprocal plot of velocity data.

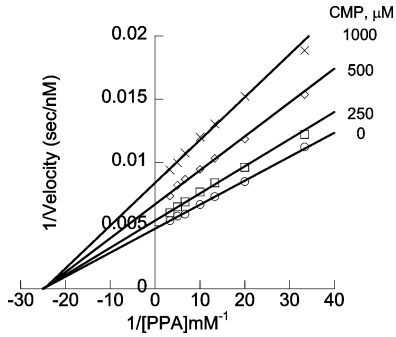

FIGURE 6: Product inhibition analysis of CMP versus PPA. Initial velocity analysis of PPCS versus varying [PPA] at different fixed [CMP] with 0.3 mM CTP and 1 mM cysteine. Double-reciprocal plot of velocity data.

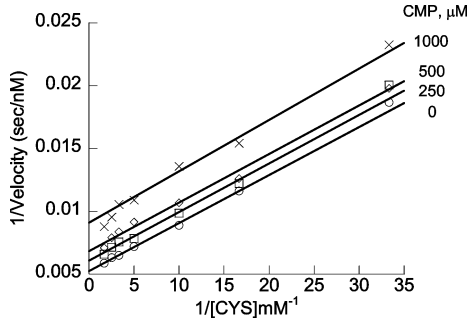

FIGURE 7: Product inhibition analysis of CMP versus cysteine. Initial velocity analysis of PPCS versus varying [cysteine] at different fixed [CMP] with 0.3 mM CTP and 0.3 mM PPA. Double-reciprocal plot of velocity data.

CTP and PPA binding. In the double-reciprocal plot of initial velocity against [CTP] at various [CMP], the fitted lines intersect on the *y*-axis, consistent with a mechanism where CMP is a competitive inhibitor with respect to CTP (Figure 5). In the double-reciprocal plot of initial velocity against [PPA] at various [CMP], the fitted lines intersect in the second quadrant, consistent with CMP as a mixed inhibitor with respect to PPA (Figure 6). Finally, in the double-reciprocal plot of initial velocity against [cysteine] at various [CMP], the fitted lines are parallel, consistent with CMP as an uncompetitive inhibitor with respect to cysteine (Figure 7). Together, the inhibition patterns are consistent with a Bi Uni Uni Bi Ping-Pong mechanism where CTP is the first substrate to bind to the enzyme and CMP is the last product to be released (Scheme 3).

The steady-state kinetic parameters determined from fitting to the initial velocity equation of a Bi Uni Uni Bi Ping-Pong mechanism, eq 2, are summarized in Table 1. The inhibition pattern of CMP with respect to the three substrates, as well as the calculated K_{iCMP} (K_{ir} in velocity equations), is summarized in Table 2.

DISCUSSION

Phosphopantothenoylcysteine synthetase catalyzes the second step of CoA biosynthesis, the amide bond formation between 4′-phosphopantothenate and L-cysteine (*7, 9*). Because of its essential nature in the growth and survival of all organisms, selective inhibitors of bacterial PPCS activity would be useful as broad spectrum antibiotics (*5, 6*). PPCS from *E. faecalis* represents a heretofore uncharacterized, new class of bacterial PPCS, found in several clinically and bioterrorism relevant pathogens, such as *Streptococcus pneumoniae* and *Bacillus anthracis* (*5, 10*). This class of enzyme is uniquely monofunctional, in that it is not natively expressed as a protein fusion with phosphopantothenoylcysteine decarboxylase as seen in a majority of bacteria. Therefore, in order to gain a more complete description of bacterial PPCS to be used in inhibitor design, the *E. faecalis* enzyme has been cloned, expressed, purified, and subjected to kinetic and isotopic labeling studies.

The *E. faecalis* enzyme shows very distant sequence similarity to the PPCS domain of the bifunctional PPCDC/PPCS proteins and, in fact, produces consistently higher similarity scores with the human monofunctional PPCS (*5, 10*). Nevertheless, our nucleotide utilization studies with the *E. faecalis* PPCS show that the enzyme is CTP-specific at physiological relevant concentrations. Thus, all bacterial PPCS enzymes characterized so far, whether expressed as a bifunctional polypeptide with PPCDC or natively expressed as a monofunctional protein, are CTP-specific. This is in stark contrast to the monofunctional human PPCS, which is reported to be ATP selective (*5*−*7*). The difference in nucleotide specificity between the bacterial and mammalian PPCS may have important implications in protein evolution and CoA regulation, as well as in developing selective bacterial PPCS inhibitors based upon differences in the nucleotide binding sites (*10, 14*).

To establish the formation of a phosphopantothenoyl cytidylate intermediate formed during the *E. faecalis* PPCS-catalyzed reaction, heteronuclear NMR was performed. ^{18}O has a significant one-bond nuclear shielding effect upon carbon and phosphorus atoms to which it is directly bonded, resulting in an observable upfield shift in the NMR resonance of such nuclei (*15*−*19*). Isotopic-shifted heteronuclear NMR has been used in the present paper to study oxygen transfer during PPCS catalysis. When *carboxyl*-^{18}O-labeled phosphopantothenate was incubated with CTP in the presence of PPCS, approximately half of the ^{18}O ended up in the phosphate group of the CMP formed. This is consistent with our kinetic mechanism wherein a phosphopantothenoyl cytidylate intermediate is formed during the first half-reaction with the release of pyrophosphate and subsequent transfer of the phosphopantothenoyl group to L-cysteine to yield phosphopantothenoylcysteine and CMP. Previous structural studies, using a mutant form of the *E. coli* PPCS domain which in noncrystallographic studies was unable to form phosphopantothenoylcysteine, also have shown a phospho-

Scheme 3

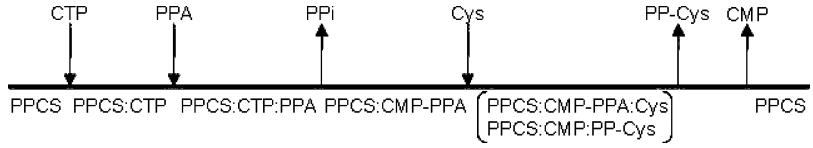

Table 1: Kinetic Parameters of PPCS at pH 7.6 and 37 °C

K_{iCTP}	$652 \pm 345\ \mu M$
K_{mCTP}	$156 \pm 17\ \mu M$
K_{mPPA}	$17 \pm 6\ \mu M$
K_{mCys}	$86 \pm 7\ \mu M$
k_{cat}	$2.9 \pm 0.1\ s^{-1}$

Table 2: Product Inhibition Patterns for PPCS

inhibitor	variable substrate	fixed substrates	pattern	calc K_{iCMP} (μM)
CMP	CTP	PPA, cysteine	comp	766 ± 90
CMP	PPA	CTP, cysteine	mixed	522 ± 23
CMP	cysteine	CTP, PPA	uncomp	732 ± 97

pantothenoyl cytidylate intermediate formed within the active site upon crystallization in the presence of CTP and PPA (*12*).

Our steady-state initial velocity and product inhibition data for *E. faecalis* PPCS fit very well with a Bi Uni Uni Bi Ping-Pong kinetic mechanism. These kinetic findings very nicely align with previous structural data from a series of crystal structures of an *E. coli* PPCS mutant (*12*). In the structural studies it was found that the dynamics of two protein loops, residues 284−299, which cover the binding site of the opposite dimer subunit, and residues 354−363, which form a pocket around the terminal phosphate on PPA, control chemical reaction as well as substrate binding and product release. In the apo form, residues 284−299 and residues 354−363 are disordered, and the cleft where PPA binds is not well formed and almost entirely solvent exposed while the CTP binding pocket is mostly formed. In the CTP bound structure, residues 284−289, 298, and 299 become ordered and interact with the binding site formed from the other dimer (*12*). As a result, the PPA binding cleft is more defined. Also, the K_d determined from isothermal titration calorimetry (ITC; see Supporting Information) matches well with the dissociation constant of CTP calculated from our kinetic studies. Thus, consistent with our kinetic results, the ITC and structural data suggest that CTP binds first and is prerequisite to PPA binding.

The Ping-Pong portion of the kinetic mechanism also correlates well with the literature. In the CTP-bound *E. coli* PPCS structure, the newly ordered Lys289 hydrogen bonds with the oxygen linking the α- and β-phosphates, serving to activate the pyrophosphate as a leaving group as well as to help orient where PPA binds to the enzyme for the subsequent attack on the α-phosphate of CTP to form the 4′-phosphopantothenoyl cytidylate intermediate. When both PPA and CTP are soaked into the crystal, the intermediate 4′-phosphopantothenoyl cytidylate is observed in the binding site, with pyrophosphate released (*12*). Our kinetic data show that PPA and cysteine have a Ping-Pong relationship, indicating that there is a product release step between the binding of PPA and the binding of cysteine. This is consistent with the release of PP_i before the substrate cysteine binds and reacts.

In the acyl cytidylate intermediate bound structure, residues 354−363 become ordered and form a pocket around the terminal phosphate, making the PPA portion of the molecule no longer solvent accessible. Likewise, the CMP-bound crystal structure obtained after all three substrates were soaked has residues 354−363 ordered, similar to the intermediate bound structure (*12*). Since CMP is still bound to the active site, while the other product phosphopantothenoylcysteine is not observed, phosphopantothenoylcysteine must be released first and CMP released last, same as the order determined via kinetics.

Overall, the enzyme mechanism of the monofunctional *E. faecalis* PPCS determined by our kinetic and isotopic studies is consistent with previous structural studies with the PPCS domain of the *E. coli* bifunctional protein. We have determined that CTP and PPA bind in an ordered fashion to the enzyme and react to form the intermediate 4′-phosphopantothenoyl cytidylate with concomitant formation of pyrophosphate. Pyrophosphate is released before L-cysteine binds and reacts with the carbonyl moiety of the mixed anhydride to form the products phosphopantothenoylcysteine and CMP in the second half-reaction. Further, product binding and substrate release are ordered, with CTP binding first and CMP released last.

ACKNOWLEDGMENT

We thank Dr. Michael McLeish and Prof. Bruce Palfey for helpful discussions.

SUPPORTING INFORMATION AVAILABLE

Isothermal titration calorimetry data, SDS−PAGE of overexpressed proteins, and nucleotide specificity assay of monofunctional PPCS. This material is available free of charge via the Internet at http://pubs.acs.org.

REFERENCES

1. Majerus, P. W., Alberts, A. W., and Vagelos, P. R. (1965) Acyl carrier protein. IV. The identification of 4′-phosphopantetheine as the prosthetic group of the acyl carrier protein. *Proc. Natl. Acad. Sci. U.S.A. 53*, 410–417.
2. Anderson, M. S., Bulawa, C. E., and Raetz, C. R. (1985) The biosynthesis of gram-negative endotoxin. Formation of lipid A precursors from UDP-GlcNAc in extracts of *Escherichia coli*. *J. Biol. Chem. 260*, 15536–15541.
3. Brozek, K. A., and Raetz, C. R. (1990) Biosynthesis of lipid A in *Escherichia coli*. Acyl carrier protein-dependent incorporation of laurate and myristate. *J. Biol. Chem. 265*, 15410–15417.
4. Magnuson, K., Jackowski, S., Rock, C. O., and Cronan, J. E., Jr. (1993) Regulation of fatty acid biosynthesis in *Escherichia coli*. *Microbiol. Rev. 57*, 522–542.
5. Gerdes, S. Y., Scholle, M. D., D'Souza, M., Bernal, A., Baev, M. V., Farrell, M., Kurnasov, O. V., Daugherty, M. D., Mseeh, F., Polanuyer, B. M., Campbell, J. W., Anantha, S., Shatalin, K. Y., Chowdhury, S. A., Fonstein, M. Y., and Osterman, A. L. (2002) From genetic footprinting to antimicrobial drug targets: examples in cofactor biosynthetic pathways. *J. Bacteriol. 184*, 4555–4572.
6. Zhang, Y. M., White, S. W., and Rock, C. O. (2006) Inhibiting bacterial fatty acid synthesis. *J. Biol. Chem. 281*, 17541–17544.

7. Brown, G. M. (1959) The metabolism of pantothenic acid. *J. Biol. Chem. 234*, 370–378.
8. Kupke, T., Uebele, M., Schmid, D., Jung, G., Blaesse, M., and Steinbacher, S. (2000) Molecular characterization of lantibiotic-synthesizing enzyme EpiD reveals a function for bacterial Dfp proteins in coenzyme A biosynthesis. *J. Biol. Chem. 275*, 31838–31846.
9. Strauss, E., Kinsland, C., Ge, Y., McLafferty, F. W., and Begley, T. P. (2001) Phosphopantothenoylcysteine synthetase from *Escherichia coli*. Identification and characterization of the last unidentified coenzyme A biosynthetic enzyme in bacteria. *J. Biol. Chem. 276*, 13513–13516.
10. Genschel, U. (2004) Coenzyme A biosynthesis: reconstruction of the pathway in archaea and an evolutionary scenario based on comparative genomics. *Mol. Biol. Evol. 21*, 1242–1251.
11. Kupke, T., Hernandez-Acosta, P., Steinbacher, S., and Culianez-Macia, F. A. (2001) *Arabidopsis thaliana* flavoprotein AtHAL3a catalyzes the decarboxylation of 4′-phosphopantothenoylcysteine to 4′-phosphopantetheine, a key step in coenzyme A biosynthesis. *J. Biol. Chem. 276*, 19190–19196.
12. Stanitzek, S., Augustin, M. A., Huber, R., Kupke, T., and Steinbacher, S. (2004) Structural basis of CTP-dependent peptide bond formation in coenzyme A biosynthesis catalyzed by *Escherichia coli* PPC synthetase. *Structure 12*, 1977–1988.
13. Ladror, U. S., Gollapudi, L., Tripathi, R. L., Latshaw, S. P., and Kemp, R. G. (1991) Cloning, sequencing, and expression of pyrophosphate-dependent phosphofructokinase from *Propionibacterium freudenreichii*. *J. Biol. Chem. 266*, 16550–16555.
14. Ostrander, D. B., O'Brien, D. J., Gorman, J. A., and Carman, G. M. (1998) Effect of CTP synthetase regulation by CTP on phospholipid synthesis in *Saccharomyces cerevisiae*. *J. Biol. Chem. 273*, 18992–19001.
15. Hansen, D. E., and Knowles, J. R. (1981) The stereochemical course of the reaction catalyzed by creatine kinase. *J. Biol. Chem. 256*, 5967–5969.
16. Hansen, D. E., and Knowles, J. R. (1982) The stereochemical course at phosphorus of the reaction catalyzed by phosphoenolpyruvate carboxylase. *J. Biol. Chem. 257*, 14795–14798.
17. Kohlbrenner, W. E., Nuss, M. M., and Fesik, S. W. (1987) ^{31}P and ^{13}C NMR studies of oxygen transfer during catalysis by 3-deoxy-D-manno-octulosonate cytidylyltransferase from *Escherichia coli*. *J. Biol. Chem. 262*, 4534–4537.
18. Dotson, G. D., Dua, R. K., Clemens, J. C., Wooten, E. W., and Woodard, R. W. (1995) Overproduction and one-step purification of *Escherichia coli* 3-deoxy-D-manno-octulosonic acid 8-phosphate synthase and oxygen transfer studies during catalysis using isotopic-shifted heteronuclear NMR. *J. Biol. Chem. 270*, 13698–13705.
19. Zheng, R., and Blanchard, J. S. (2001) Steady-state and pre-steady-state kinetic analysis of *Mycobacterium tuberculosis* pantothenate synthetase. *Biochemistry 40*, 12904–12912.

BI802240W